Organic &
Biomolecular
Chemistry

Cite this: *Org. Biomol. Chem.*, 2011, **9**, 4467

www.rsc.org/obc

PAPER

Rhodamine-based probes for metal ion-induced chromo-/fluorogenic dual signaling and their selectivity towards Hg(II) ion†

Bamaprasad Bag* and Ajoy Pal

Received 15th December 2010, Accepted 7th March 2011
DOI: 10.1039/c0ob01179g

The new signaling probes **2–6**, rhodamine-B derivatives of various receptors which contain different donor atoms for effective metal ion coordination, were synthesized and their absorption as well as fluorescence spectral responses were evaluated in the presence of various metal ions. All these probes along with the reference probe **1** have exhibited optimal metal ion-induced absorption and fluorescence enhancement with Hg(II) ion in the longer wavelength region (>500 nm) in MeCN, exploiting the spectral characteristics of metal ion-induced structural transformation of rhodamine. The selectivity and sensitivity towards Hg(II) ion were better pronounced in MeCN–H_2O (1 : 1 v/v) medium, implying the role of the solvent molecules, water in particular, in the preferential Hg(II) coordination environment. Complexation of Hg(II) to **1–6** not only enhanced the absorption at ~560 nm, which turned the colourless solution into pink to facilitate a naked eye detection, but also amplified the fluorescence intensity simultaneously to offer high sensitivity of detection at lower concentration. The Hg(II)-induced photo-physical spectral responses of **1–6** in presence of other competitive metal ions rendered their high selectivity towards Hg(II). Further, their reversible dual channel signaling pattern under the action of counter anions, exploiting coordination tendency of anions towards Hg(II), which compete with probe-metal interaction, implied the reversibility in their Hg(II) coordination. The selectivity, sensitivity and reversibility, in principle, establishes the potential of these probes as chemosensors for Hg(II) ion detection.

Introduction

Transition and heavy metal ions play a predominant role[1] in many biological processes in living systems, apart from their extensive domestic and industrial utility. Despite being essential for bio-systems, their absence or presence in excess of the requisite amount can lead to various physiological disorders. Further, their presence in the environment as pollutants and, thus, their toxic effects that pose severe health hazards are matters of concern.[2] Thus, selective detection of such important yet hazardous metal ions at the sub-micromolar level for biological, environmental and clinical purposes is highly desirable and indispensable. Although various analytical methods, such as atomic absorption and emission spectrometry, inductively coupled plasma mass spectroscopy, neutron activation analysis, X-ray fluorescence spectrophotometry, *etc.*, have been employed to detect these metal ions, synthetic probes which exhibit signal transduction upon analyte binding, metal ions in particular, find wide-domain utility and impact as chemical sensors in biomedical and environmental research and as molecular logics in molecular information processing. The design and synthetic perspective of such probes involve various methodological designs, perturbation of involved photo-physical processes and manifestation of output signal. Designed through various combinations of receptor, spacer and signaling subunits, these miniaturized supramolecular architectures respond to chemical information changes occurring in the receptor unit upon analyte binding and communicate the information through perturbation of operative photophysical processes to be measured at the signaling sub-unit. Chromogenic signaling probes offer a naked eye detection of analytes as the output signal modulation appears as a mode of color change or variation in absorption. Fluorescent-signaling probes have proven to be essential and powerful tools to monitor *in vitro* and/or *in vivo* biologically relevant species such as metal ions due to their advantages over the other analytical methods in terms of sensitivity, high selectivity, shorter response time, non-complicated sampling, non-destructive and non-invasive properties, and offer real-time monitoring of the processes occurring at different time scales. Although heavy and transition metal ions quench fluorescence *via* the spin-orbit coupling effect, a large number of fluorescent probes[3] have been reported for these metal ions that overcome their inherent quenching nature through a suitable design of the probe. Most of these reported fluorescent turn-on probes for metal ions exhibit

Colloids and Materials Chemistry Department, Institute of Minerals and Materials Technology (CSIR), P.O.: R.R.L., Bhubaneswar, 751013, India. E-mail: bpbag@immt.res.in

† Electronic supplementary information (ESI) available: ^{1}H-, ^{13}C-NMR, ESI-MS spectra of the probes **1–6**, their absorption and emission spectral data in various solvents, in presence of various metal ions at different operational conditions. See DOI: 10.1039/c0ob01179g

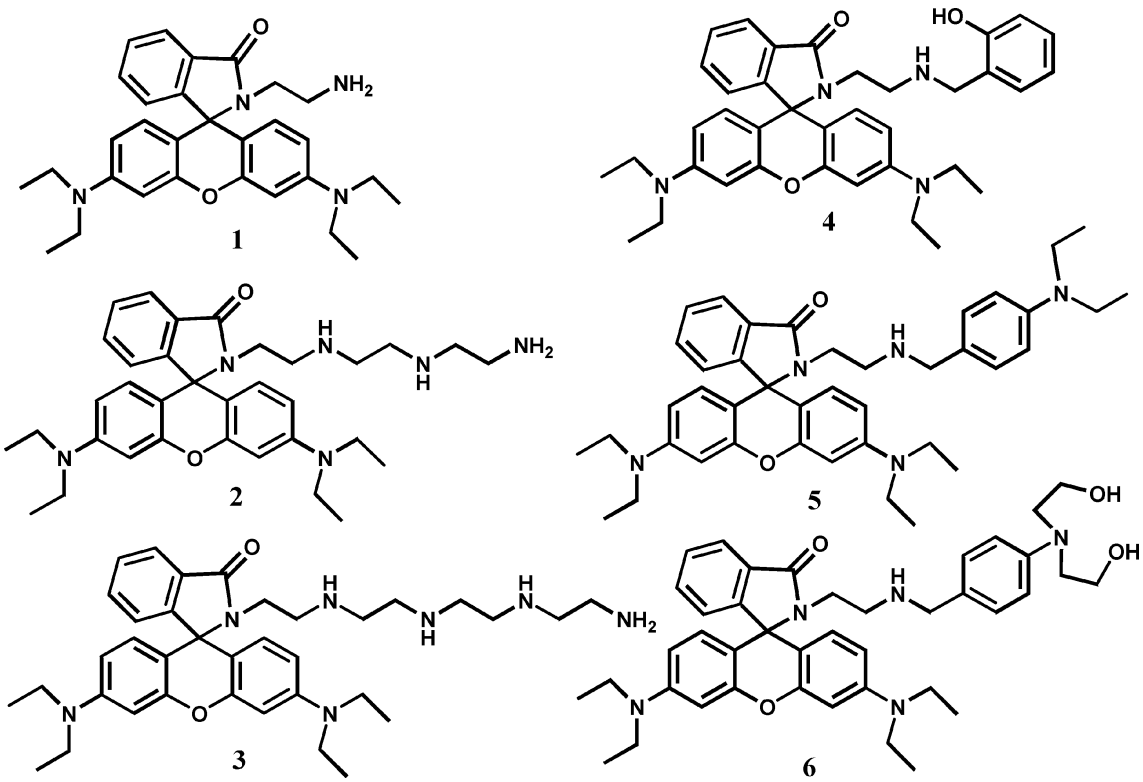

Scheme 1 Schematic representation of the probes **1–6**.

chelation-enhanced fluorescence enhancement in organic media, responsive towards several metal ions or even exhibit a restricted detection limit. Hence, the quest for development of new signaling probes for metal ions still pertains to the selectivity and sensitivity issue. In this context, it should be advantageous to design probes that facilitate both chromogenic as well as fluorogenic signaling upon selective analyte binding.

The excellent spectroscopic properties of rhodamine dye, such as high absorption coefficient, high fluorescence quantum yield, absorption and emission at longer wavelength, *etc.*, have re-oriented the focus on designing rhodamine-based probes[4] for various analytes, which also offer the advantageous virtue of their ability to exhibit optical signal modulation in aqueous media. Various rhodamine-based chromogenic and fluorogenic chemosensors have recently been developed for selective detection of many transition and heavy metal ions such as Hg(II),[5–7] Cu(II),[8] Fe(III),[6j,9] Cr(III),[9h,10] Pb(II),[6j,11] Ag(I),[5f] Au(III),[12] Pd(II),[13] Eu(III)[14] *etc.*. The signaling mechanism of these probes follows a straight forward protocol, *i.e.* the colourless and non-fluorescent spirocyclic rhodamine structurally equilibrates to the colored and highly fluorescent ring-opened amide form in the presence of a metal ion. The rhodamine-based probes exert simultaneous chromogenic and fluorogenic signaling as they not only exhibit excellent enhancement in absorption and fluorescence intensity in response to metal ion binding, but also develop a strong colour as a signature of the sensing event to facilitate naked eye detection. The selectivity, sensitivity, operational conditions and reversibility are the vital parameters to be manifested for any metal ion selective probe; hence, the modular design of the receptor which is responsible for metal ion binding plays a crucial role. As the receptor provides a number of donor atoms for effective metal ion coordination, the nature and selectivity of a probe can be tailored by the selection of appropriate donor atoms at strategic positions with a varied ligand design topology to accommodate a particular ion. Thus, in rhodamine-based signaling probes for metal ions, receptor subunits with varied spatial disposition of donor atoms in a covalent framework may be envisaged to exhibit different selectivity towards different metal ions.

With this strategic design, we have synthesized rhodamine-based probes (**1–6**, Scheme 1) with different receptor units which impart different stereo-electronic environments for effective metal-probe interaction. Further, their dual channel fluorogenic and chromogenic signaling in response to various metal ions have been the focus of investigation in order to develop real-time monitoring protocols for selective detection of these ions. These new probe molecules (**2–6**) exhibit highly Hg(II)-selective chromogenic and fluorogenic signaling among all the metal ions investigated. The probe **1**, for which the synthesis has been reported[6i,8l] earlier, also shows maximum absorption and fluorescence enhancement in the presence of Hg(II) ion. In the context of mercury contamination,[15] its toxicity, subsequent biological and environmental impacts[16] and the recent increasing interest to develop Hg(II)-selective rhodamine based probes[5–7] *etc.* has instigated a protocol to design such probes with high selectivity, sensitivity and reversibility in a simple synthetic route to contribute significantly towards development of an easy to handle method for real-time monitoring of mercury concentration in biological and environmental samples.

Results and discussion

The rhodamine derivatives **1–3** were synthesized by derivatization of rhodamine-B hydrochloride with ethylene diamine, triethylene tetramine and tetraethylene pentamine, respectively, in ethanol. Although **1** has been reported earlier as a precursor to various rhodamine-based probes,[6i,8l] to the best of our knowledge the detailed photophysical behavior and their signal modulation with various metal ions have not been elaborately studied. The probes **4–6** were synthesized through Schiff-base condensation of **1** with 2-hydroxy benzaldehyde, 4-(diethylamino)benzaldehyde and 4-(*N*,*N*-bis(2-hydroxyethyl)amino)benzaldehyde, respectively, in ethanol followed by reduction with $NaBH_4$. The compounds were characterized by ^{1}H-NMR, ^{13}C-NMR and ESI-MS. The characteristic peak near ~66 ppm (9-carbon) in ^{13}C-NMR spectrum of the compounds in $CDCl_3$ confirms that the rhodamine exists in its spirolactam conformation. The absorption and emission spectral properties of **1–6** in various solvents with varying polarity such as n-hexane, 1-propanol, chloroform, dichloromethane, tetrahydrofuran, ethyl acetate, acetone, *N*,*N*-dimethylformamide, dimethylsulfoxide, methanol, ethanol and acetonitrile were investigated. As the reversible lactonization-delactonization process of rhodamine highly depends on the organic solvent media or pH, the signaling responses of these probes in different pH and in organic aqueous media were also carried out. The solutions of **1–6** in acetonitrile/acetonitrile–water binary mixtures are colourless and non-fluorescent, which supports rhodamine's predominant existence in spirolactam form.

Absorption and emission pattern of 1–6

The absorption of the probes (**1–6**) observed at ~315 nm and ~270 nm in all the solvents under investigation were due to ligand localized π–π* transitions and found to be slightly solvatochromic ($\Delta\lambda = 10$ nm) in nature. The molar extinction coefficient (ε) of these transitions varied with the nature of the substituent attached to the rhodamine moiety. The absence of any absorption transition at 400–600 nm region (Fig. 1) and appearance of the colorless solution ascertained rhodamines lactonized conformation in these compounds. On the other hand, their emission spectral patterns (Fig. 1) upon excitation at 350–500 nm region, which were taken after averaging ten measurements, were found to be rather complicated with three emission peaks at ~540, ~560 and ~580 nm attributed to those of the lactonized rhodamine. The observed quenched emissions of **1–6** (fluorescence quantum yield $\phi_{FT} < 0.001$) in almost all the solvents were contributed to by combined influential factors: (a) rhodamines existence in spirolactam form which facilitates an efficient intersystem crossing and (b) operative photo-induced electron transfer processes from distal donor groups present in their receptor moiety. Though quenched, the emission quantum yields (ϕ_F) of all these compounds expectedly varied with solvent polarity function. The fluorescence emissions of **1–6** were more pronounced in protic solvents such as MeOH, EtOH and 1-PrOH in comparison to aprotic solvents, which may be attributed to the solvent-assisted ring-opening of the spiro-structure in traces of the probes in protic environment, as also observed in other rhodamine-based probes.[9i]

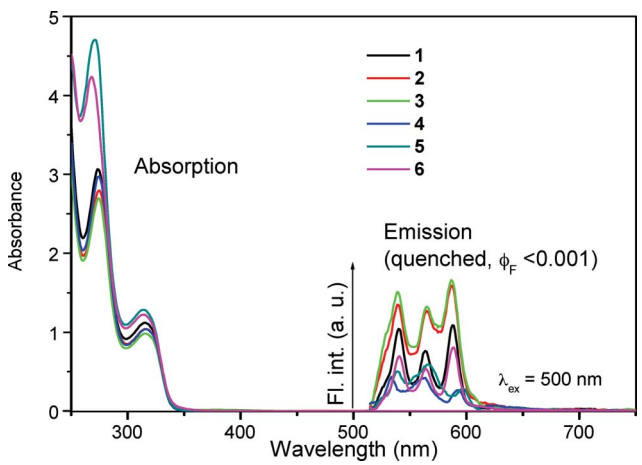

Fig. 1 Absorption (1×10^{-4} M) and emission (1×10^{-6} M, λ_{ex} = 500 nm) spectral pattern of **1–6** in MeCN.

Absorption spectral pattern of 1–6 in the presence of various metal ions

As the probes **1–6** contain different receptor units with varying spatial disposition of donor atoms attached to the rhodamine moiety and are expected to have a different binding mode with various metal ions exploiting spatial compatibility for optimal overlap and effective metal–ligand interaction; various metal ions such as Na(I), K(I), Mn(II), Fe(II), Co(II), Ni(II), Cu(II), Zn(II), Pb(II), Ag(I), Cd(II) and Hg(II) were added to the solution of **1–6** in MeCN to investigate the effect of metal ion addition on absorption in visible wavelength region (400–650 nm window). As observed, the UV-Vis spectra of **1–6** in MeCN exhibited no absorption in the 400–700 nm region due to rhodamine spiro-conformation in solutions, however, addition of metal ions lead to appearance of a strong absorption transition at ~560 nm with a shoulder at ~515 nm (Fig. 2a & b) in all the probes, which is characteristic of rhodamine-based dyes. Metal ion addition also resulted in a colour change in the solution of the probes in MeCN, from colourless to pink, which implies a metal-induced delactonization of rhodamines initial spirolactam form to its ring-opened amide conformation that facilitates the complexation. Among all the metal ions investigated, all the probes exhibited maximum absorption enhancement ($\varepsilon_{M.L}/\varepsilon_L$) and subsequent colourless→pink colour transition in presence of Hg(II) ions yielding a significantly high absorption (ε = 2.3 × 10^4–4.2 × 10^4 dm^3 mol^{-1} cm^{-1}) at ~560 nm in MeCN. A few of the metal ions such as Pb(II) and Fe(II) also have induced an appreciable enhancement in absorption at ~560 nm, though to a significantly lower extent in comparison to that of Hg(II), whereas the rest of the metal ions induced a negligible absorption change. The extent of absorption enhancement at ~560 nm in the presence of metal ions varies with nature of the probe, type of the metal ion and their binding interactions, because the spatial disposition of the donor atoms of receptor units and the structural rigidity of probes facilitate different coordination environment towards different metal ions. The absorption enhancement factor ($\Delta\varepsilon_{\sim 560}$) at ~560 nm of **1–6** upon Hg(II) coordination were found to be as high as 3588, 2311, 2126, 3683, 2503 and 2330-fold respectively (Fig. 3). Next to Hg(II), Pb(II) exhibited relatively higher absorption at 550 nm upon complexation among other metal ions with **1**, **2**, **3**, **4** and **6** resulting in respective 941, 618, 1068, 1731 and 705-fold enhancement. The

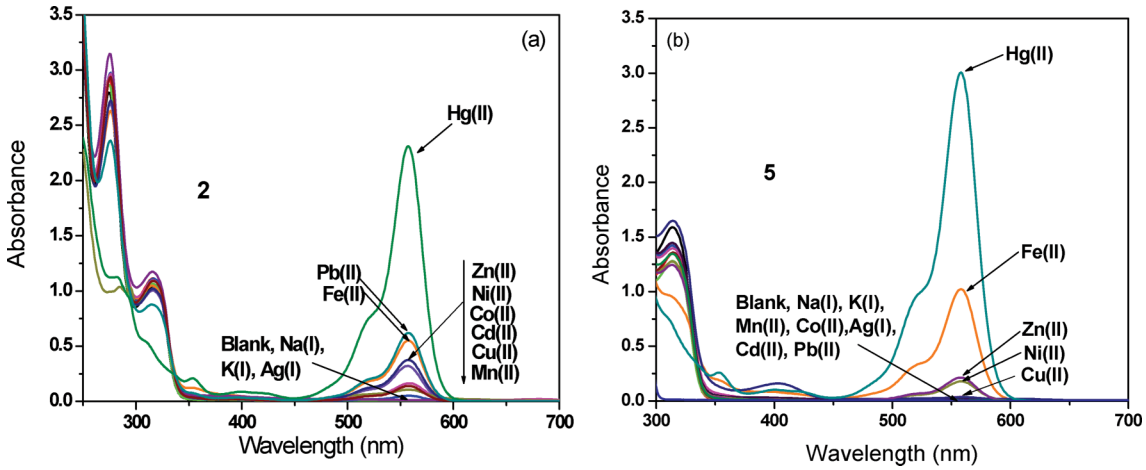

Fig. 2 Absorption spectra of (a) **2** (1×10^{-4} M) and (b) **5** (1×10^{-4} M) in MeCN in the absence and presence of various metal ions.

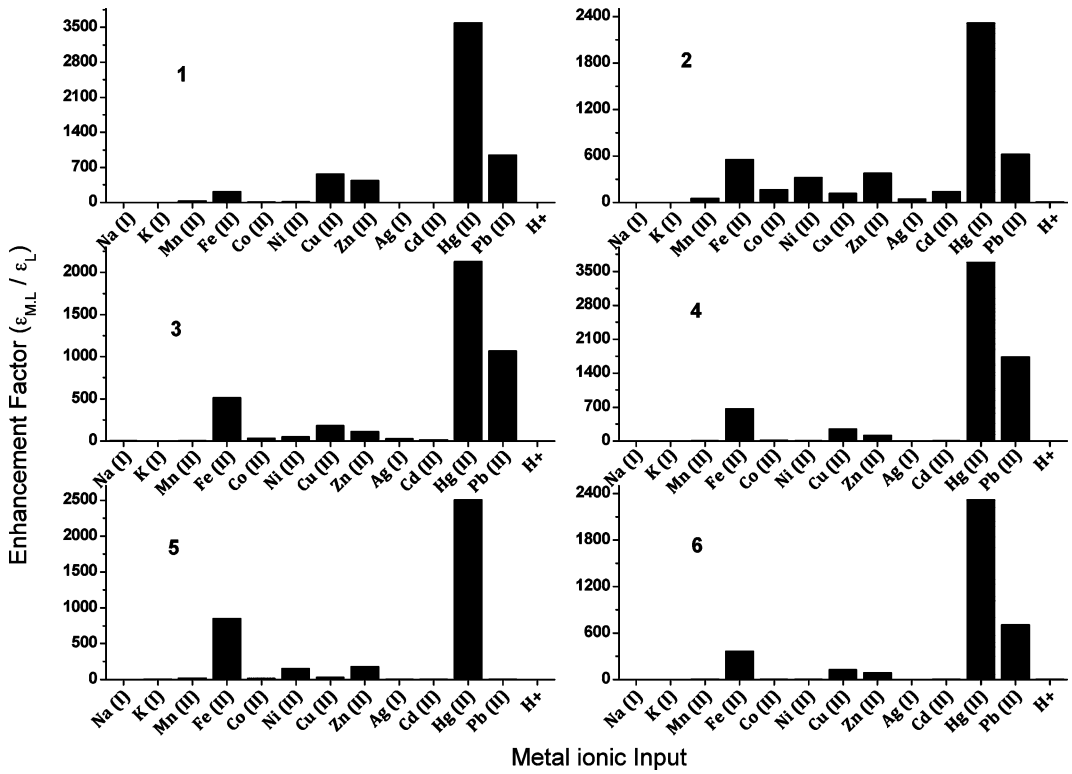

Fig. 3 Absorption enhancement factor of **1–6** (10 μM) in the presence of various metal ions (50 μM) in MeCN.

absorption ($A_{\sim 560}$) of **5** did not enhance with Pb(II), implying a non-coordinating environment of the probe towards that particular metal ion, while Fe(II) enhanced its absorption up to 853-fold. The $\Delta\varepsilon_{560}$ due to complexation with other metal ions in comparison to that with Hg(II) indicates that all these probes preferably facilitate an efficient coordination environment for Hg(II) ion.

When investigated in acetonitrile : water (1 : 1 v/v) medium rather than in acetonitrile, the absorption ($\varepsilon_{\sim 560}$) at ~560 nm of **2–6** increased selectively in presence of Hg(II) ion among all the metal ions investigated and subsequent pink colour development was also observed (Fig. 4c & d). However, similar Hg(II)-selectivity could not be observed for the probe **1** in MeCN–H_2O (1 : 1 v/v) mixture although the absorption enhancement($\Delta\varepsilon_{\sim 560}$) was found to be more pronounced with Hg(II) in comparison to other metal ions, as observed in the case of MeCN. In order to verify the influence of water molecules on Hg(II)-selective chromogenic signaling in **2–6**, the metal ion-induced changes in absorption in these probes were investigated in different acetonitrile–water binary mixtures of varied proportions (9 : 1, 7 : 3 and 1 : 1 v/v). Interestingly, the chromogenic signaling behavior of all these probes implies that their selectivity towards Hg(II) ion enhanced gradually with increase in water proportion in acetonitrile–water binary mixture. Other metal ions such as Pb(II) and Fe(II), which induced a small enhancement in absorption in all the probes (except in **5**, where Pb(II) did not exhibit any change) in MeCN, failed to exhibit such absorption enhancement in MeCN–H_2O

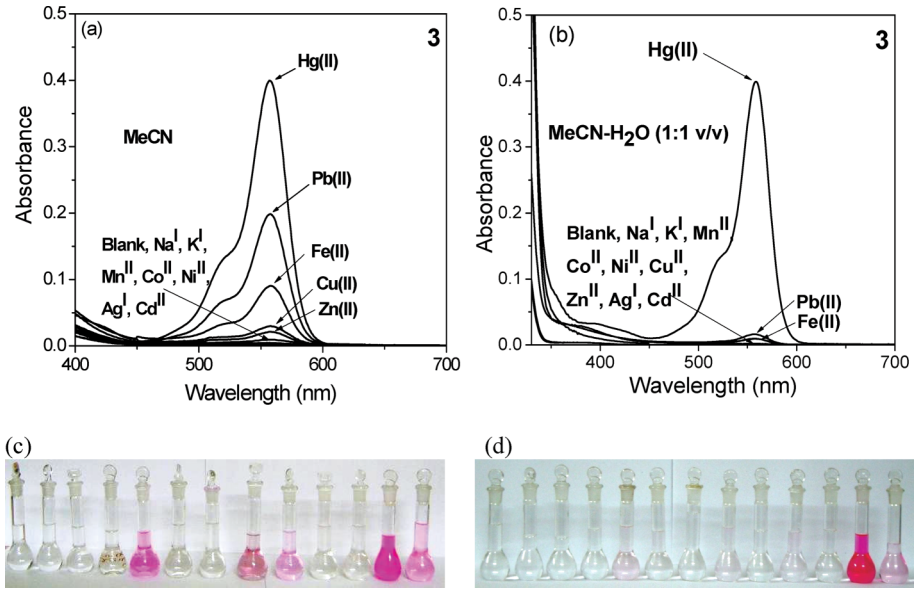

Fig. 4 Absorption spectra of **3** (1.8×10^{-5} M) in (a) MeCN and (b) MeCN–H_2O (1 : 1 v/v) in absence and presence of various metal ions. The colour changes of **6** (10 μM) in response to various metal ions (100 μM) in (c) MeCN and (d) MeCN–H_2O (1 : 1 v/v). The colour change due to added metal ions to the solution are in the order of blank, Na(I), K(I), Mn(II), Fe(II), Co(II), Ni(II), Cu(II), Zn(II), Ag(I), Cd(II), Hg(II) and Pb(II) (from left to right).

(1 : 1 v/v) medium. The suppression of chromogenic signaling pattern of Pb(II) and Fe(II) in organic–aqueous medium may be attributed to a restricted metal ion–probe interaction in the presence of water molecules.

The time-course studies for each of the probes with Hg(II) revealed that the complexation induced colour change attained optimal absorbance in almost 1 min and remained constant for at least 24 h. As the high selectivity of any probe towards a particular metal ions is conferred by reduced or negligible interference of other competitive metal ions, the change in absorption of **1–6** due to Hg(II) were also investigated in presence of other metal ions in both MeCN and MeCN–H_2O media. It was observed that Hg(II) ion still produces a change in absorption in the presence of other cations in probes **2–6** almost similar to that in their absence, which implies the high selectivity of the probes towards Hg(II) ion. Thus, the unique feature of selective Hg(II)-induced absorption amplification and subsequent colour change enables the probes **2–6** to potentially be employed for naked-eye detection of Hg(II) within a concentration threshold.

The plot of absorbance at 560 nm of **1–6** as a function of mole fraction of added metal ions (Jobs plot) in MeCN as well as MeCN–aqueous medium reveals that these probes bind to the metal ion in different stoichiometry depending upon their covalent architecture. The probe–metal stoichiometries were found to be 1 : 1 for probes **1** and **4**, 1 : 2 for probes **2**, **3** and **6**, while a peculiar ratio of 1 : 1.5 was observed for probe **5**, which implies a different binding mode of each probe towards the metal ions added, Hg(II) in particular. The 1 : 1.5 probe–metal complexation stoichiometry arises when at least two probe molecules (**5**) bind to three metal ions (Hg(II) and Fe(II)) during complexation. The UV-vis absorption titration of **1–6** (1.0×10^{-4} M–1.0×10^{-5} M) with various metal ions (1.0×10^{-6} M–1.0×10^{-3} M) were carried out in MeCN as well as in MeCN–H_2O (1 : 1 v/v), which have shown an appreciable change in absorption and subsequent colour transition. Apart from metal ion-induced increase in absorption (A_{-560}) at different concentrations of metal ions in all the titration plots of different probe–metal combination, the increase in absorption peak at 354 nm, which is attributed to the perturbation of associated $\pi \rightarrow \pi^*$ transitions, and a distinct isosbestic point at ~330 nm in the absorption spectra indicate formation of a single component upon complexation, *i.e.* coordinated delactonized rhodamine. The absorption spectral pattern of **2**, **3** and **6** on titration with different equivalents of Hg(II), Pb(II) and Fe(II) in MeCN revealed that absorption attains a maximum upon addition of 2 equiv. of metal ions (Fig. 5) and remains constant up to addition of 10 equiv. of the cation. Further, it was observed from the titration plots that the absorption maximum (A_{-560}) of the probes remains almost the same up to addition of 1 equiv. of metal ion and subsequent addition up to 2 equiv. leads to its gradual enhancement to

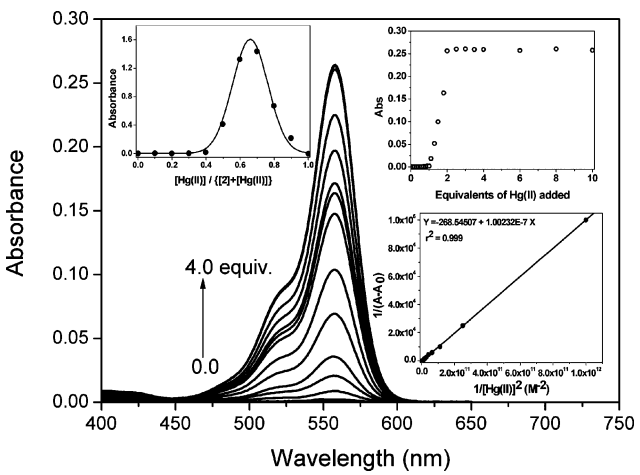

Fig. 5 Absorption spectra of the titration of **2** (1×10^{-5} M) with different amount of Hg(II) added in MeCN–H_2O (1 : 1 v/v). Inset: Jobs plot, absorption as a function of Hg(II) added and change in absorption of **2** at 557 nm as a function of Hg(II) concentration.

attain the maximum, which indicates that these probes first bind to the metal ion through distal donor atoms of their respective receptor units yielding almost no change in absorption response, then followed by coordination at delactonized rhodamine unit which results in increased $A_{\sim 560}$ and brings about the colour change. A similar observation in the absorption titration plots for **2**, **3** and **6** with Hg(II) in MeCN–H_2O(1 : 1 v/v), where these probes exhibit selectivity towards Hg(II) among all the metal ions investigated, have indicated towards their 1 : 2 binding mode which were well supported by respective Jobs plots. The complex stability constants (K_s) for Hg(II) coordination, determined through Benesi–Hildebrand method[7] for 1 : *n* stoichiometry as a reciprocal of the slope of the linear regression of the plot of $1/\Delta A$ *vs.* $1/[\mathrm{Hg(II)}]^n$ were found to be 0.99×10^7, 3.02×10^8 and 1.01×10^7 M^{-2} with **2**, **3** and **6**, respectively ($n = 2$, $r^2 > 0.99$). The higher K_s values for these probes correlate to their covalent architecture, *i.e.* the number of available coordination sites in the receptor. When titrated with Hg(II) or Fe(II), the absorption of **5** (10 μM) attained maximum with addition of 1.5 equiv. of metal ion and remained constant up to 20 equiv. further addition. The linear regression of the plot for determination of K_s did not fit with a good correlation (correlation coefficient < 0.7) with 1 : 1 or 1 : 2 stoichiometry of **5**⊂Hg(II) complex (either $n = 1$ or $n = 2$), rather exhibited a good correlation with 1 : 1.5 complex stoichiometry and its K_s with Hg(II) was estimated to be 1.06×10^5 $M^{-1.5}$ ($n = 1.5$, $r^2 > 0.99$), which supports the complex stoichiometry pattern as deduced by the Jobs plot. Similarly, absorption titration of **4** (10 μM) with Hg(II)/Pb(II)/Fe(II) in MeCN and that of **1** (10 μM) with Hg(II) indicated towards a 1 : 1 complexation stoichiometry, as observed in respective Jobs Plots. The K_s of Hg(II) coordination in MeCN–H_2O (1 : 1 v/v) was determined to be 1.20×10^4 M^{-1} for **4** while it was 5.73×10^4 M^{-1} for **1**. The determined K_s values for Hg(II) coordination with these probes in MeCN–H_2O (1 : 1 v/v) revealed that **3**, which incorporates a higher number of amino donor sites in its architecture, has a higher binding affinity towards Hg(II). The observable naked eye detection of the pink colour development in these probes (μM) upon Hg(II) addition have a detection limit of $0.3–0.5 \times 10^{-6}$ M of Hg(II).

The absorption titration profiles suggested that addition of excess of metal ions (>100 equivalents of that of probe) to the solution of probes ($>1 \times 10^{-5}$ M) lead to decrease in the metal-induced enhanced absorption. The absorption titration spectra of **5** (3×10^{-4} M) with Fe(II) in MeCN revealed that the absorption at 558 nm enhanced to attain maximum, though small in comparison to that with Hg(II), remained constant up to addition of 50 equiv. of Fe(II) and gradually decreased upon further addition (>100 equiv.). Apart from that, a new absorption peak simultaneously appeared at 470 nm and gradually enhanced with further increase in Fe(II) concentration exhibiting a clear isosbestic point at 500 nm. The absorption transition of **5** at 470 nm in presence of excess of Fe(II) may be attributed to a ligand–metal charge transfer band, which arises due to a different, but preferential, binding mode of **5** with Fe(II) when present in excess. Except Fe(II) addition to **5**, similar absorption peak appearance could not be observed for any other metal ions when added in excess to any of the probes.

Emission spectral pattern in presence of metal ions

The fluorescence spectral pattern of **1–6** when excited in the 500–550 nm region in the presence of various metal ions in MeCN revealed that their non-fluorescent solution becomes highly fluorescent with enhancement of fluorescence intensity at ~580 nm emission maximum (λ_{em}^{max}) upon metal addition (Fig. 6). This implies a delactonization process, induced by metal ion coordination, of the non-fluorescent spirocyclic form of rhodamine to its highly fluorescent ring opened form, a primitive characteristic of rhodamine dye. The extent of chelation-enhanced fluorescence effects were found to depend highly upon nature of the probes and interacting metal ions. Among all the metal ions investigated, these probes exhibited high fluorescence enhancement at λ_{em}^{max} = ~580 nm (fluorescence quantum yield ϕ_{FT} = 0.464–0.659) in the presence of Hg(II) ion in MeCN with 970, 579, 725, 1315, 1773 and 510-fold fluorescence intensity enhancement factors (F/F_0) respectively in **1–6**. Among all the probes, **5** exhibited maximum Hg(II)-induced fluorescence enhancement (F/F_0 > 1700-fold), showing its higher affinity towards Hg(II) in comparison to other probes. Barring Hg(II), only addition of Pb(II) and Fe(II) ions promote a small increase in F/F_0 in these probes (except for **5** where Pb(II) did not change the fluorescence intensity) in MeCN, while other metal ions failed to respond with a similar appreciable change in fluorescence under identical conditions. The fluorescence enhancement factor and corresponding quantum yields of **1–6** in the presence of various metal ions are collected in Table 1. When investigated in MeCN–H_2O binary mixtures (9 : 1, 7 : 3, 1 : 1 v/v), the selectivity of **2–6** towards Hg(II) ion enhances with an increase in the water proportion in the solvent mixture, as also observed with absorption change. Thus in MeCN–H_2O (1 : 1 v/v) medium, all these probes exhibited high fluorescence enhancement selectively in presence of Hg(II) while their fluorogenic signaling behavior with Pb(II) and Fe(II) observed in MeCN were suppressed, and other metal ions exhibited no or negligible change in fluorescence emission. In order to verify the selectivity of these probes towards Hg(II) ions over other competitive metal ions, the fluorescence intensity change (F/F_0) of **1–6** (1 μM) upon addition of Hg(II) (10 μM), other metal ions (10 μM), and Hg(II) along with different metal ions in both MeCN and MeCN–H_2O (1 : 1 v/v) were evaluated. The Hg(II) addition to the solution of **1–6** enhanced the fluorescence intensity up to same extent (error <5%) in either presence or absence of other interfering cations in both the solvent conditions, while other

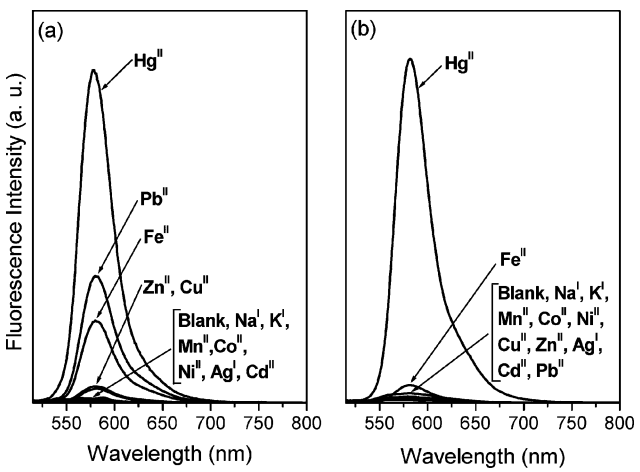

Fig. 6 Fluorescence spectra (λ_{ex} = 500 nm) of **6** (1 μM) in presence of various metal ions (5 μM) in (a) MeCN and (b) MeCN–H_2O (1 : 1 v/v).

Table 1 Absorbance, emission enhancement factor and corresponding quantum yields of the probes in presence of various metal ions[a]

Probe	Ionic Input	Absorbance (log ε)		Emission EF (I_F/I_F^0)		Quantum yield (ϕ_{FT})	
		MeCN	MeCN–H_2O (1 : 1 v/v)	MeCN	MeCN–H_2O (1 : 1 v/v)	MeCN	MeCN–H_2O (1 : 1 v/v)
1	Blank	1	1	1	1	<0.001	<0.001
	Na(I)	1.146	1.112	~1	1	<0.001	<0.001
	K(I)	1.114	1.085	1.2	1	<0.001	<0.001
	Mn(II)	2.512	2.501	1.4	1	<0.001	<0.001
	Fe(II)	3.331	3.176	30.9	21.3	0.015	0.009
	Co(II)	1.973	1.932	3.7	1.7	~0.002	0.001
	Ni(II)	2.170	2.101	6.6	2.9	0.003	0.002
	Cu(II)	3.757	3.725	70	62.2	0.035	0.021
	Zn(II)	3.637	3.619	52.5	47.7	0.026	0.026
	Ag(I)	1.176	1.119	5.2	2.8	~0.003	~0.003
	Cd(II)	1.447	1.389	4.4	1.9	~0.002	~0.002
	Hg(II)	4.555	4.132	970.4	897.6	0.485	0.392
	Pb(II)	3.974	3.883	255	207.2	0.127	0.102
	H^+	1.556	3.155	~1	71.5	<0.001	0.023
2	Blank	1	1.024	1	1	0.001	<0.001
	Na(I)	1.342	1.062	2.1	1.2	<0.002	<0.001
	K(I)	1.079	1.044	2.1	1.6	<0.002	<0.001
	Mn(II)	2.706	1.098	1.2	0.9	~0.001	<0.001
	Fe(II)	3.741	1.505	93.1	3.22	0.077	~0.002
	Co(II)	3.215	1.995	22.7	1.86	0.019	<0.001
	Ni(II)	3.505	1.267	31.1	2.5	0.029	0.002
	Cu(II)	3.067	1.229	32.5	3.7	0.030	0.003
	Zn(II)	3.574	1.004	39.4	0.9	0.033	0.001
	Ag(I)	2.640	1.217	1.4	1.3	~0.001	<0.001
	Cd(II)	3.144	1.516	2.2	0.9	~0.002	<0.001
	Hg(II)	4.364	3.979	579.3	339.5	0.475	0.258
	Pb(II)	3.791	1.893	100.6	12.5	0.083	0.007
	H^+	1.708	3.669	1	67.8	~0.001	0.021
3	Blank	1.041	1	1	1	0.001	<0.001
	Na(I)	1.532	1.041	1.1	1.01	~0.001	<0.001
	K(I)	1.114	1.011	1.2	1.02	~0.001	<0.001
	Mn(II)	1.568	1.009	4.2	0.97	0.004	<0.001
	Fe(II)	3.694	2.677	103.3	2.39	0.094	0.002
	Co(II)	2.526	1.132	1.6	1.03	~0.002	<0.001
	Ni(II)	2.725	1.213	1.3	0.95	~0.001	<0.001
	Cu(II)	3.229	1.699	16.1	2.69	0.015	~0.002
	Zn(II)	3.099	1.994	10.5	1.34	0.010	<0.001
	Ag(I)	2.438	1.126	9.5	1.01	0.010	<0.001
	Cd(II)	2.210	1.227	3.5	0.98	0.003	<0.001
	Hg(II)	4.346	4.347	725.3	448.6	0.659	0.366
	Pb(II)	4.044	2.963	148.6	9.37	0.135	0.008
	H^+	1.380	3.615	~1	61.3	~0.001	0.020
4	Blank	1.041	1	1	1	<0.001	<0.001
	Na(I)	0.903	0.998	~1	1.07	<0.001	<0.001
	K(I)	1.176	1.051	~1	1.05	<0.001	<0.001
	Mn(II)	1.799	1.034	1.6	1.02	<0.001	<0.001
	Fe(II)	3.865	2.214	214	23.59	0.107	0.010
	Co(II)	2.114	1.997	8.4	1.04	0.004	<0.001
	Ni(II)	2.013	1.198	4.4	0.91	0.002	<0.001
	Cu(II)	3.196	2.221	55.1	2.24	0.028	0.001
	Zn(II)	3.118	2.179	49.7	1.35	0.025	0.001
	Ag(I)	1.176	1.319	2.8	0.94	<0.001	<0.001
	Cd(II)	1.756	1.551	2.9	0.91	<0.001	<0.001
	Hg(II)	4.608	4.499	1315.5	1038.6	0.658	0.479
	Pb(II)	4.280	3.276	685.9	15.9	0.342	0.008
	H^+	1.204	4.063	~1	98.8	<0.001	0.042
5	Blank	1.079	1.003	1	1	<0.001	<0.001
	Na(I)	1.380	1.104	1.4	1.02	<0.001	<0.001
	K(I)	1.568	1.226	3.7	1.1	0.001	<0.001
	Mn(II)	2.354	2.004	22.2	1.2	0.007	<0.001
	Fe(II)	4.011	3.009	361.9	22.6	0.109	0.006
	Co(II)	2.260	1.018	20.3	1.2	0.006	<0.001
	Ni(II)	3.256	2.176	73.5	1.2	0.022	<0.001
	Cu(II)	2.553	3.029	36.7	2.6	0.011	<0.001
	Zn(II)	3.332	2.011	72.6	10.4	0.022	0.002

Table 1 *(Contd.)*

Probe	Ionic Input	Absorbance (log ε)		Emission EF (I_F/I_F^0)		Quantum yield (ϕ_{FT})	
		MeCN	MeCN–H_2O (1 : 1 v/v)	MeCN	MeCN–H_2O (1 : 1 v/v)	MeCN	MeCN–H_2O (1 : 1 v/v)
	Ag(I)	1.505	1.339	2.5	1.4	<0.001	<0.001
	Cd(II)	1.833	1.523	1.9	1.2	<0.001	<0.001
	Hg(II)	4.478	4.402	1773.3	1360.6	0.532	0.364
	Pb(II)	1.732	3.024	1.3	1.5	<0.001	<0.001
	H^+	1.389	3.747	1	114.7	<0.001	0.049
6	Blank	1	1	1	1	<0.001	<0.001
	Na(I)	1.079	1.014	1.4	1	~0.001	<0.001
	K(I)	1.146	1.037	1.4	1.2	~0.001	<0.001
	Mn(II)	2.013	1.882	1.1	1.6	~0.001	<0.001
	Fe(II)	3.822	2.673	98.4	9.6	0.089	0.007
	Co(II)	1.681	1.463	1	1.4	~0.001	<0.001
	Ni(II)	2.072	1.839	1.3	2.1	~0.001	<0.001
	Cu(II)	3.364	2.322	30.7	7.9	0.028	0.002
	Zn(II)	3.198	2.047	25.4	1.3	0.023	<0.001
	Ag(I)	1.602	1.274	1.1	1	~0.001	<0.001
	Cd(II)	1.699	1.359	1.2	1.3	~0.001	<0.001
	Hg(II)	4.624	4.058	510.8	443.2	0.464	0.366
	Pb(II)	4.108	2.833	159.9	22.1	0.145	0.016
	H^+	1.690	3.348	1	32.6	~0.001	0.019

[a] Experimental conditions: Absorption: [probes] = 1×10^{-6}–1×10^{-5} M; [metal ion] = 1×10^{-4} M; MeCN. Emission experimental conditions: concentration of free probe: 1×10^{-6}–1×10^{-8} M; added metal ion = 1×10^{-6} M; λ_{ex} = 500 nm; excitation and emission band-pass: 5 nm; T = 298 K; MeCN. The error in ϕ_F is within 5%. EF: The enhancement factors are in comparison to that of corresponding metal free probes.

metal ions did not induce any significant change. This establishes the significant feature of high selectivity of these probes towards Hg(II) over other competitive metal ions.

The fluorescence titration profile of **1–6** (1.0×10^{-7} M) *versus* various concentration of Hg(II) in MeCN–H_2O (1 : 1 v/v) revealed that fluorescence intensity of these probes with λ_{em}^{max} at 580 nm enhanced significantly with gradual increase in Hg(II) concentration and remained constant thereafter saturation of complexation within a concentration threshold. Fluorescence spectral pattern of **2** (1 μM) in MeCN–H_2O(1 : 1 v/v) upon addition of various concentrations of Hg(II) is given in Fig. 7. The other probes were also exhibited similar titration profile with Hg(II). The fluorescence enhancement factor (F/F_0) were proportional to the concentration of Hg(II) added ([Hg(II)] = 1.0×10^{-8} M–1.0×10^{-6} M) to each of the probes. The complex stability constants for Hg(II) coordination with **1–6** were estimated to be 2.62×10^6 M^{-1}, 3.83×10^{12} M^{-2}, 6.60×10^{13} M^{-2}, 8.99×10^8 M^{-1}, 4.18×10^{10} $M^{-1.5}$ and 1.08×10^{12} M^{-2}, respectively, (error < 5%) on the basis of linear fitting (inset, Fig. 7) of the double reciprocal plot of fluorescence intensity $[1/\{(F/F_0) - 1\}]$ as a function of concentration of Hg(II) added $\{1/[\text{Hg(II)}]^n\}$. The good coefficient ($r^2 > 0.99$) of linear regression for the assigned complex stoichiometry was also well supported by their corresponding binding mode as obtained through Jobs plots and absorption titration pattern. From the titration data of the probe **5** with Hg(II), it was observed that linear regression of the plot for determination of K_s did not fit with a good correlation (correlation coefficient <0.6–0.8) with 1 : 1 or 1 : 2 stoichiometry of **5**Hg(II) complex (either $n = 1$ or $n = 2$), but rather exhibited a good correlation with 1 : 1.5 complex stoichiometry, similar to that observed in the case of absorption titration. The fluorescence enhancement factors and subsequent higher K_s values (>10^7) for **1–6** with Hg(II) corresponding to their higher binding ability suggested that these probes have the potential to detect

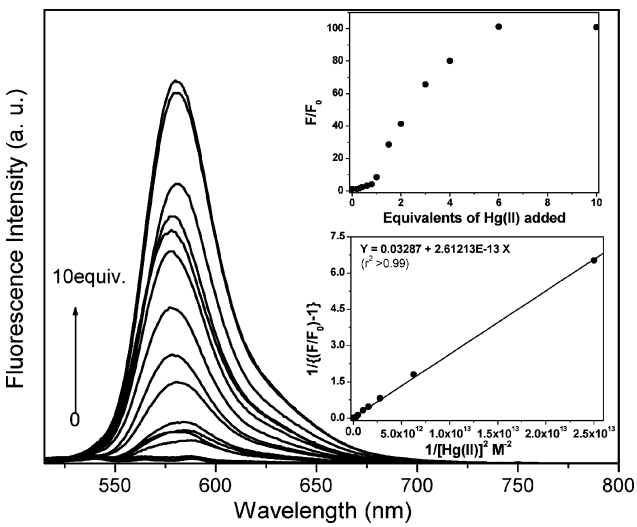

Fig. 7 Fluorescence spectral pattern of **2** (1 μM) in MeCN–H_2O (1 : 1 v/v) upon addition of various concentrations of Hg(II). Each spectrum was taken after 1 min of Hg(II) addition. Inset (top): Fluorescence enhancement change (normalized with the emission of free probe **2**) as a function of equivalents of Hg(II) added. Inset (bottom): Linear regression plot of fluorescence intensity change $1/\{(F/F_0) - 1\}$ as a function of concentration $1/[\text{Hg(II)}]^2$ M^{-2}.

Hg(II) ion at a very low concentration level. Based on their fluorescence signal modulation, the detection limit (fluorescence signal S/N = 3) for Hg(II) were measured to be very low (3.0×10^{-8} M–5×10^{-9} M) and comparable to those of Hg(II)-selective rhodamine-based probes,[5t,6l,8l] and even with other receptor-based probes.[17] The fluorescence signal responses, in comparison to that of absorption, induce higher sensitivity of these probes towards Hg(II) coordination. Moreover, the essential factor for a probe in

chemo-sensing application is the real-time monitoring of analyte concentration. The time course studies for each of the probes with Hg(II) revealed that the probe–metal complexation occurred in almost 1 min, as reflected through maximum fluorescence intensity change, and remained constant for at least 12 h.

Reversibility in signaling responses

The reversibility is an important aspect of any probe to be employed as a chemical sensor for detection of specific metal ions. To investigate the reversibility in chromo- and fluorogenic signaling of **1–6** rendered by Hg(II) complexation, ammonium salts of different anions such as SO_4^{2-}, NO_3^-, PO_4^{3-}, CO_3^{2-}, SCN^-, Cl^-, F^-, I^-, OAc^- and HCO_3^- were added to the solution containing the probe and Hg(II), and their absorption and fluorescence intensity change were monitored after 1 min. Among all the anions, the enhanced absorption due to Hg(II) coordination to the probe immediately reduced upon addition of acetate and iodide with subsequent disappearance of pink colour of the solution to colourless. Simultaneously, the enhanced fluorescence was also quenched to exhibit a signal with fluorescence intensity almost equal to that of a metal-free probe. This implies that these anions have a higher coordinating tendency towards Hg(II) and thus replace the probes to bind with the metal ion. Similar diminishing signaling patterns of the Hg(II)-complexed probes were also observed with Cl^- after 12 h of addition of the anion. The absorption and emission spectral pattern of the solution containing **3** and Hg(II) upon addition of various anions is given in Fig. 8. Other probes also responded similarly to establish reversible chromo- and fluorogenic signaling of Hg(II) ion as a function of counter anions. The lowered absorption and emission intensity due to anion addition was observed to enhance again upon further addition of Hg(II), turning the colour of the solution from colourless to pink, which suggests the possibility of reuse of these probes as chemosensors for selective Hg(II) detection. Apart from anions, a few chelating agents and the probes themselves were also added to the Hg(II)–probe complex in MeCN–H_2O (1 : 1 v/v) medium in order to verify the reversibility in Hg(II)-induced absorption and emission signaling responses. It was observed that the amplified absorption and emission due to selective Hg(II) coordination to the probe also decreases substantially upon addition of chelating agents such as ethylenediamine-tetraacetic acid (EDTA) with simultaneous change in colour from pink to colourless. When the probe itself is added to the saturated solution containing Hg(II)–probe complex, a negligible decrease in absorption and emission spectral intensity of the Hg(II)–probe complex was observed due to a concentration variation of the probe in the solution.

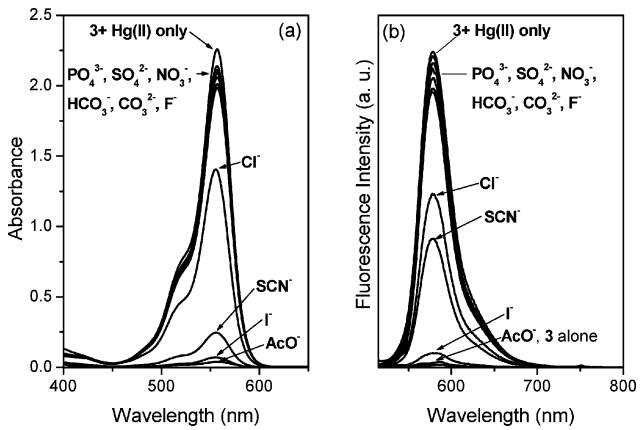

Fig. 8 Change in (a) absorption and (b) fluorescence intensity upon addition of various anions (10 equiv.) to the solution containing **3** (1 equiv.) and Hg^{II} (5 equiv.). Conc. of **3** = 1.0×10^{-4} M (abs) and 1.0×10^{-8} M (em). λ_{ex} = 500 nm.

The photophysical spectral behaviours of **1–6** monitored in different pH have shown that no observable change in absorption and fluorescence intensity occur in pH 7.0 to 10.0, which indicates that these probes can potentially be used in biological systems. However, their enhanced absorption and fluorescence intensity proportional to the decreased pH (<7.0) revealed that delactonization of the rhodamine spiro-ring occurred under acidic conditions even in absence of any metal ion. When monitored at pH 4.0 in comparison to that in basic or neutral pH (10.0–7.0), appearance of the absorption peak at 557 nm (ε_{557} = 5637, 4678, 1563, 2580, 245 and 6624 $dm^3\ mol^{-1}\ cm^{-1}$ respectively for **1–6**) and pink colour of the solution was observed for all the probes. Simultaneously, a ~40 nm red-shift in fluorescence maxima along with an enhancement in intensity ($F_{pH4.0}/F_{pH7.0}$ > 10-fold) was also observed. In this context, a negligible change in absorption or fluorescence intensity of these probes was observed in presence of H^+ ($HClO_4$) in MeCN. However, when H^+ was added to their solution in EtOH, MeOH and even in acetonitrile–aqueous medium (9 : 1, 7 : 3 and 1 : 1 v/v), the absorption ($A_{\sim 560}$) and fluorescence (F/F_0) were substantially enhanced. This implies a hindrance of protonation-induced delactonization of the rhodamine spiro-ring in these probes in aprotic solvents like MeCN, which gets facilitated in protic solvents. Both absorption and fluorescence changes in the presence of metal ions in MeCN revealed that **2–6** promoted significant signal amplification in the presence of Hg(II) while a few other metal ions such as Fe(II) and Pb(II) also induced smaller changes. It may be argued that the hydrated metal perchlorate salts are known to generate protons in organic solvents, and hence might be contributing to the turn-on signaling responses of these probes in the presence of metal ions through proton-induced delactonization of the spirolactam ring. However, if the proton generation in the medium by the metal salts were responsible, then the extent of enhancement should have been almost the same in all the cases. The signaling responses of these probes in MeCN–H_2O (1 : 1 v/v) indicated their Hg(II) selectivity where other metal ions impart no or negligible spectroscopic changes (Fig. 9 & Table 1). Similar water-mediated tuning of selectivity towards Hg(II) could not be observed in **1**, although it has exhibited optimal fluorogenic and chromogenic signal amplification in the presence of Hg(II) among all the metal ions investigated. The reason for enhanced Hg(II) selectivity of **2–6** may be rather complicated, however the possibility of solvent molecules playing the crucial role in metal–probe complexation may not be overlooked. MeCN being a coordinating solvent, it actively indulges in complexation of Hg(II) as well as with a few other metal ions with these probes through solvent-assisted coordination apart from the probes binding to the metal ion. The coordination of other metal ions to these probes in the presence of water molecules is restricted due to their strong hydration ability, whereas only Hg(II) coordination to **2–6** gets facilitated in acetonitrile–aqueous medium to exhibit a Hg(II)-selective absorption signal amplification with change in colour

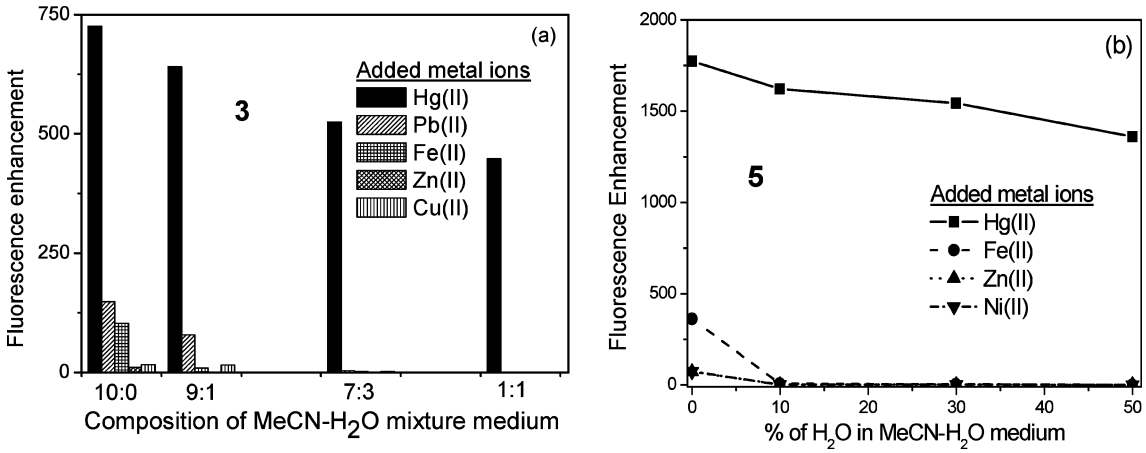

Fig. 9 Fluorescence enhancement of (a) **3** and (b) **5** in the presence of various metal ions in various compositions of MeCN–H_2O binary mixture as medium. (Conc. of ligand = 1×10^{-6} M, conc. of metal = 1×10^{-5} M, RT, λ_{ex} = 500 nm.)

from colourless to pink (increased $A_{\sim 560}$) and simultaneous fluorescence enhancement. Further, in order to determine the better probe in terms of selective Hg(II) sensing among **2–6**, a controlled experiment was carried out with addition of Hg(II) to a solution containing all these competitive probes (equimolar proportion) in MeCN–H_2O (1 : 1 v/v) medium. Both the absorption and emission intensity of the mixture solution was enhanced ($F/F_0 \approx 1300$-fold) to the extent of that of just **5** upon Hg(II) addition under similar experimental conditions, which implied that the selective Hg(II) sensing was better observed in **5** among all these probes.

Structure–function correlation

Although the new probes **2–6** were expected to exhibit chromogenic and fluorogenic signaling selectively in the presence of different metal ions, due to their structural variation in the rhodamine-appended receptor, which provides different binding sites for complexation, rather interestingly **1–6** have shown optimal spectroscopic response preferentially with Hg(II). The Hg(II) selectivity of these probes might be due to their common structural feature, *i.e.* the substituted amino-ethyl-amido-phenyl segment of the ring-opened rhodamine, which coordinates selectively to Hg(II) and is responsible for metal ion-induced enhanced absorption and fluorescence signals modulation. Hence, the substituted amino-ethyl moiety in all these probes, when appended to rhodamine, provided an optimal stereo-electronic situation for effective Hg(II) coordination irrespective of the nature of the substituent and rendered subsequent spectral responses for selective Hg(II) detection. In this regard, the absorption spectral pattern of **5** in the presence of Cu(II) in various compositions of MeCN–H_2O medium has provided vital evidence (Fig. 10a). The Cu(II) induced absorption of the ring-opened rhodamine at 557 nm ($\varepsilon = 3950$ dm^3 mol^{-1} cm^{-1}), though much lower than that in the presence of Hg(II), was reduced significantly while the absorption transition at 478 nm (ε = 18 306 dm^3 mol^{-1} cm^{-1}) along with its vibronic structures observed in MeCN subsequently increased with the increase in aqueous composition in organic–aqueous binary mixtures with an isosbestic point at 508 nm. Excitation of the (0,0) transition at 478 nm and its vibronic structures did not exhibit any emission, whereas excitation of that due to ring-opened rhodamine exhibited

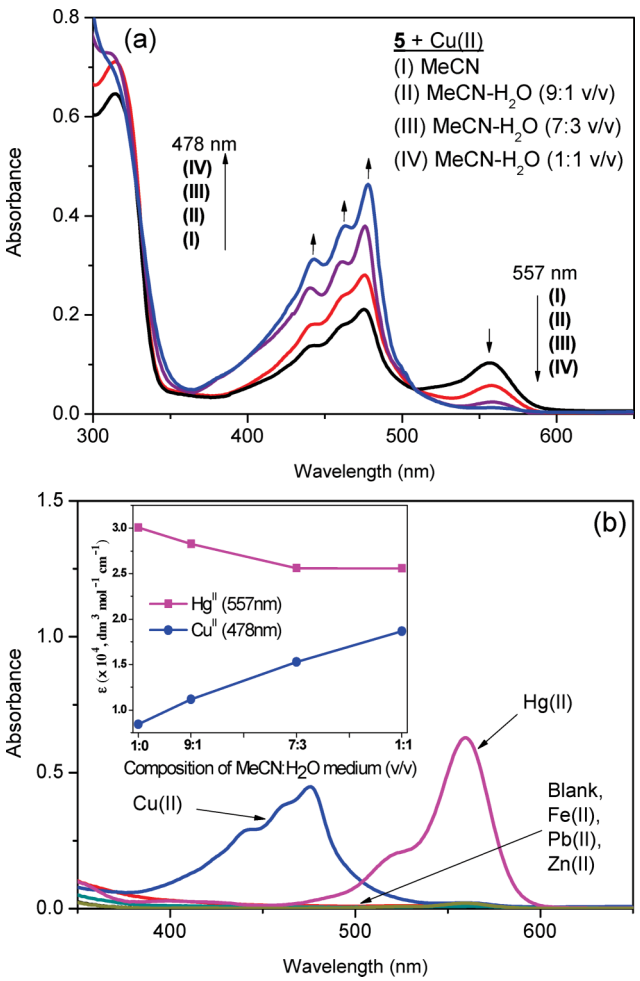

Fig. 10 (a) Absorption spectral responses of **5** (2.5×10^{-5} M) in presence of Cu(II) ion (1×10^{-4} M) in various composition of MeCN–H_2O mixture as medium. (b) Absorption spectra of **5** (2.5×10^{-5} M) in the presence of various metal ions in MeCN–H_2O (1 : 1 v/v). Inset: Metal ion-induced absorption modulation as a function of composition of medium.

a fluorescence emission at ~580 nm. The Cu(II)-induced absorption at 478 nm thus may be assignable to a ligand-to-metal charge

transfer transition which arises due to binding of Cu(II) to the distal N atom of the phenyl-amino-ethyl unit of **5**. The increase in Cu(II)-induced LMCT band and subsequent reduction of ring-opened rhodamine absorption with an increase in the amount of the aqueous component in the binary composition of the medium implied that the presence of water gradually restricts the ability of Cu(II) to delactonize the spiro-ring of rhodamine, and rather promoted the metal ion to bind preferentially at the distal amino end. It has been observed here that the probe **5** exhibited an altered chromogenic signaling selectively with two different metal ions when monitored at two different output wavelengths (Fig. 10b). Its absorption spectral pattern in the presence of various metal ions in MeCN–H_2O (1 : 1 v/v) revealed that the absorption peak at 557 nm enhanced ($\varepsilon = 25\,569$ dm^3 mol^{-1} cm^{-1}) selectively in presence of Hg(II) with a colour change from colourless to pink, while that at 478 nm enhanced ($\varepsilon = 18\,671$ dm^3 mol^{-1} cm^{-1}) selectively in the presence of Cu(II) with a colour change from colourless to yellow. The altered signaling responses of a probe selective towards two different inputs when monitored at two different output channels contribute significantly towards development of transducers that perform complex chemical logic action.

To verify the coordination geometry around the substituted amido-ethyl-amino unit of these probes upon complexation and their preferential binding to Hg(II) ion, geometrical optimization calculations of a model system containing the same binding unit and its complexes with various metal ions were performed at DFT level with the Gaussian 09 program[18] using B3LYP/6-31G* basis set for ligand and B3LYP/LANL2DZ basis set for metal ions, which includes relativistic small-core effects with effective core potential. The non-bonded N_{amino}–O_{amido} distances of the model system and its corresponding metal complexes revealed that Hg(II) ion favorably fits to the chelation cavity of amido-ethyl-amino receptor unit in comparison to other metal ions. Its correlation with these probes, which contain the same donor sites for effective metal ion binding, may arguably support that a preferential Hg(II) coordination by these probes leads to subsequent metal ion-induced delactonization of the rhodamine spiro-ring resulting in optimal Hg(II)-mediated chromo- and fluorogenic signaling among all the metal ions investigated. The other binding sites on the receptor attached to amino-ethyl-amido-rhodamine unit might not be contributing to the selective Hg(II)-induced spiro-ring opening, and subsequent coordination for effective signaling, however, contributes significantly towards the sensitivity of the Hg(II) detection by these probes providing increased complex stability. In this context, it has been found that for the 4-[(*N*,*N*-bis(2-hydroxyethyl)amino)phenyl receptor, when attached to the rhodamine-ethyl-amino-methyl unit, the photo-physical spectral pattern of the probe **6** has shown selectivity towards Hg(II), however a 4,4-difluoro-4-bora-3a,4a-diaza-*s*-indacene (BODIPY) derivative of the same receptor unit has been reported[19] to exhibit fluorogenic signaling selective with Pb(II). Similarly, a rhodamine B derivative of triethyl tetramine (probe **2**) exhibited Hg(II)-selective spectral responses, while a rhodamine 6G derivative of the same receptor unit has been reported[9h] to exhibit Cr(III)-selective signaling. Emphasis on the structural pattern would have beneficially contributed to understand the Hg(II)-selective signaling behaviours of these probes through structure–function correlation before a conclusion can be put forward regarding its coordination environment; however, all attempts to obtain X-ray quality crystals of **1–6** with Hg(II) remained unsuccessful. Nevertheless, based on the photo-physical signaling responses, the new probes **2–6** can potentially be employed for qualitative and quantitative detection of Hg(II) in real-time sensing in environmental aspects.

Conclusion

In summary, the new rhodamine-based signaling probes **2–6**, designed and synthesized through a simple synthetic route by condensation of different receptors containing amino/oxo donor atoms in their architecture with rhodamine-B, have been shown to exhibit both fluorogenic and chromogenic signalling induced by metal ions, exploiting the structure–function correlation of rhodamine. Among all the metal ions under investigation, Hg(II)-induced optimal signal amplification. All these probes not only exhibited maximum absorption enhancement in the presence of Hg(II) and turned the colour of the solution from colourless to pink with an observable naked eye detection limit of 0.3–0.5 $\times$ 10^{-6} M of Hg(II) concentration, but also simultaneously exhibited optimal Hg(II)-induced amplification of fluorescence intensity to two orders in magnitude with lower detection limit ($<3 \times 10^{-8}$ M). A few other metal ions such as Pb(II) and Fe(II) have also induced appreciable absorption and emission enhancement though much lower in comparison to that due to Hg(II). The selectivity of **2–6** enhanced towards Hg(II) in organic–aqueous binary mixture medium, implying a vital role of water molecules in regulating the coordination environment of complexation which modulates the signalling pattern, whereas the reference probe **1** failed to exhibit Hg(II) selectivity under similar conditions. As other competitive metal ions promote no or negligible change in absorption and fluorescence intensity and induced negligible interference in Hg(II)-induced observable and detectable spectral changes, these probes facilitate high selectivity towards Hg(II). The spectral response of each probe towards Hg(II) varied with their structural design, which incorporates different binding sites on their receptor unit, exploiting their binding affinity and different binding modes of complexation. Among all the probes, **5** exhibited optimal signaling responses in terms of Hg(II) sensing. The spectral response of **1–6** towards Hg(II) was found to be reversible with addition of counter anions such as iodide or acetate, which establishes these probes to be chemosensors for Hg(II). Considering the advantages of high sensitivity, selectivity, reversibility and real-time response of **2–6** towards Hg(II), these probes might potentially be used for environmental analysis or *in vitro* Hg(II) detection in living cells. Our subsequent work will be focused along this direction.

Materials and methods

All the reagent grade chemicals were used without purification unless otherwise specified. Rhodamine-B hydrochloride, ethylenediamine, triethylene tetramine, tetraethyl pentamine, 2-hydroxybenzaldehyde, 4-(diethylamino)benzaldehyde, 4-(*N*,*N*-bis(2-hydroxyethyl)amino)benzaldehyde and the metal perchlorate salts were obtained from Aldrich (USA) and used as received. Anhydrous sodium sulfate, acids, buffers and the solvents were received from S. D. Fine Chemicals (India). All the solvents were freshly distilled prior to use for fluorescence measurements by

following the literature procedures[20] and all the reactions were carried out under N_2 atmosphere. Chromatographic separations were done by column chromatography using 100–200 mesh silica gel.

The compounds were characterized by elemental analyses, ^{1}H-NMR, ^{13}C-NMR and mass (ESI) spectroscopy. ^{1}H-NMR and ^{13}C-NMR spectra were recorded on a JEOL JNM-AL400 FT V4.0 AL 400 (400 MHz and 100 MHz, respectively) instrument in $CDCl_3$ with Me_4Si as the internal standard. Electrospray mass (ESI) spectral data were recorded on a MICROMASS QUATTRO II triple quadruple mass spectrometer. The dissolved samples of the compounds in suitable solvents were introduced into the ESI source through a syringe pump at the rate of 5 μL min^{-1}, ESI capillary was set at 3.5 kV with 40 V cone voltage and the spectra were recorded at 6 s scans. The DART-MS were recorded on a JEOL-AccuTOF JMS-T100LC mass spectrometer having a DART source. Melting points were determined with a melting point apparatus by PERFIT, India and were uncorrected. Elemental analyses were done in an Elementar Vario EL III Carlo Erba 1108 elemental analyzer. UV-visible spectra were recorded on a Perkin Elmer Lambda 650 UV/VIS spectrophotometer at 298 K in 10^{-4}–10^{-6} M concentration. Steady-state fluorescence spectra were obtained with a Fluoromax 4P spectrofluorometer at 298 K. Fluorescence quantum yields were determined as per the procedure reported earlier from our laboratory.[21] All the samples were excited at 500 nm only to compare their uncorrected spectra with that of rhodamine-G in ethanol[22] as standard (ϕ_F = 0.95) for determination of fluorescence quantum yields. The detection limit of the metal ion was determined by a procedure reported in literature.[23]

The complex stability constants (K_s) were determined from the change in absorbance or fluorescence resulting from the titration of dilute solutions (~10^{-4}–10^{-6} M) of the probes against metal ion solution following the Benesi–Hildebrand method[7] for a complexation of 1 : n probe : metal stoichiometry as depicted in the eqn(1)

$$\frac{1}{X - X_0} = \frac{1}{K_S(X_{max} - X_0)[M(II)]_0^2} + \frac{1}{X_{max} - X_0} \quad (1)$$

where X_0 is the absorbance or fluorescence of the probes at a particular wavelength, X is the absorbance or fluorescence intensity obtained with added [M(II)], A_{max} is the absorbance or fluorescence obtained with excess amount of metal ion added and $[M(II)]_o$ is the concentration of metal ion added. The double reciprocal plot of absorption or fluorescence spectral change $(1/X - X_0)$ as a function of added metal ion concentration $(1/[M]^n)$ results in a linear regression and its slope determines K_s (M^{-n}).

Synthesis

Compound 1, aminoethyl rhodamine. This compound was synthesized following the procedure reported[6i,8k,21] earlier.

Compound 2. To a stirring solution of rhodamine B hydrochloride (0.478 g, 1 mmol) in EtOH (50 mL), triethylene tetramine (0.7 mL, 5 mmol, excess) in EtOH (20 mL) was added dropwise and allowed to react under reflux condition for 15 h until the colour of the solution changes from pink to orange. The solution was then cooled to room temperature, filtered and the solvent was removed under reduced pressure. Water (30 mL) was added to the pale yellow solid and extracted with $CHCl_3$ (330 mL). The combined organic layers, after drying over anhydrous Na_2SO_4, were evaporated under reduced pressure to obtain **2** as a pale brown solid. It was further purified by passing through a column (100–200 mesh silica gel) with chloroform and methanol mixture (98 : 2 v/v). Yield: 0.43 g (76%); mixed mp: 112–114 °C; ESI-MS, m/z^+ (%): 571 [**2**]$^+$ (45%); ^{1}H-NMR (400 MHz, $CDCl_3$, 25 C, TMS, δ): 7.80 (br s, 1H), 7.35 (t, J = 3.99 Hz, 1H), 7.22 (br s, 1H), 7.0 (br s, 1H), 6.34 (d, J = 7.99 Hz, 2H), 6.30 (s, 2H), 6.20 (d, J = 3.99 Hz, 2H), 3.25 (d, J = 3.99 Hz, 8H), 2.75 (br s, 2H), 2.61 (br s, 2H), 2.51 (br s, 8H), 2.30 (br s, 4H), 1.08 (t, J = 7.99 Hz, 12H); ^{13}C-NMR (100 MHz, $CDCl_3$, 25 C, TMS, δ):168.51, 153.13(d), 148.64, 132.27(d), 130.98(t), 128.55(d), 127.94, 123.65, 122.57, 107.95, 105.36(t), 97.56, 64.77(d), 50.94, 48.47, 48.05, 47.47, 44.20, 40.73, 39.85, 12.44; anal. calcd for $C_{34}H_{46}N_6O_2$: C, 71.55, H, 8.12, N, 14.72%; found: C, 71.46, H, 8.21, N 14.63%.

Compound 3. To a stirring solution of rhodamine B hydrochloride (0.478 g, 1 mmol) in EtOH (50 mL), tetraethylene pentamine (1 mL, 5.25 mmol, excess) was added and the reaction mixture was heated to reflux for 12 h with constant stirring until the colour of the solution changes from pink to orange. The solution was then cooled to room temperature, filtered and the solvent was removed under reduced pressure. $CHCl_3$ (30 mL) was added to the light brown semi-solid and washed thoroughly with water (330 mL). The organic layer, after drying over anhydrous Na_2SO_4, was evaporated under reduced pressure to obtain a pale brown semisolid as desired product. It was further purified by passing through a column (100–200 mesh silica gel) with chloroform and methanol (97 : 3 v/v) as eluent. Yield: 0.44 g (72%); ESI-MS, m/z^+ (%): 614 [**3**]$^+$ (53%); ^{1}H-NMR (400 MHz, $CDCl_3$, 25 C, TMS, δ): 7.79 (br s, 1H), 7.38 (br s, 1H), 7.00 (br s, 1H), 6.33 (s, 2H), 6.30 (br s, 1H), 6.21 (br s, 2H), 6.03 (br s, 2H), 3.26 (br s, 13H), 3.02 (br s, 2H), 2.72 (br s, 2H), 2.64 (br s, 2H), 2.53 (br s, 10H), 1.08 (br s, 12H); ^{13}C-NMR (100 MHz, $CDCl_3$, 25 C, TMS, δ):168.49, 153.56, 153.31, 148.75 (d), 132.44, 131.13, 129.01, 128.76, 128.05, 123.81, 122.75, 108.08, 105.53, 97.71(d), 65.01, 60.96, 57.80, 53.15 (d), 50.57, 47.65, 45.81, 44.37, 40.02, 38.64, 12.60; anal. calcd for $C_{36}H_{51}N_7O_2$: C, 70.44, H, 8.37, N, 15.97%; found: C, 70.29, H, 8.58, N 15.82%.

Compound 4. To a completely dissolved solution of **1** (0.5 g, 1.03 mmol) in EtOH (40 mL), 2-hydroxy benzaldehyde (0.2 mL, 1.9 mmol) was added and allowed to react at room temperature for 24 h. with constant stirring. $NaBH_4$ was the added to the reaction mixture to reduce the Schiff base thus formed. It was further allowed to react for 2 h at room temperature with constant stirring to ensure the complete reduction. The solvent was evaporated to dryness under reduced pressure. Water (30 mL) was added to the pale yellow solid and extracted with $CHCl_3$ (330 mL). The combined organic layers, after drying over anhydrous Na_2SO_4, were evaporated under reduced pressure to obtain the crude product, which was further purified by column chromatography ($CHCl_3$–MeOH = 95 : 5 v/v) to obtain **4** as a pale yellow solid. Yield: 0.48 g (79%); mixed mp: 82–85 C; DART-MS, m/z^+ (%): 591.3 [**4** + 1]$^+$ (100%); ^{1}H-NMR (400 MHz, $CDCl_3$, 25 C, TMS, δ): 7.91 (d, J = 7.99 Hz, 1H), 7.44 (t, J = 3.99 Hz, 1H), 7.10 (m, 2H), 6.86 (d, J = 3.99 Hz, 1H), 6.79 (d, J = 7.99 Hz, 1H), 6.69 (t, J = 7.99 Hz, 2H), 6.40 (d, J = 7.99 Hz, 2H), 6.36

(d, J = 3.99 Hz, 2H), 6.22 (d, J = 7.99 Hz, 2H), 3.80 (s, 2H), 3.28–3.34 (br s, 10H), 2.51 (s, 2H), 1.15 (br s, 12H); ^{13}C-NMR (100 MHz, $CDCl_3$, 25 C, TMS, δ): 169.92, 159.23, 153.42, 149.58, 134.24, 132.29, 129.13, 129.01, 124.84, 124.26, 119.62, 116.73, 108.09, 106.11, 97.54, 65.62, 52.48, 47.71, 44.48, 39.18, 12.53; anal. calcd for $C_{37}H_{42}N_4O_3$: C, 75.23, H, 7.17, N, 9.48%; found: C, 73.09, H, 7.27, N 9.32% [$C_{37}H_{42}N_4O_3 \cdot H_2O$].

Compound 5. To a stirring ethanolic (40 mL) solution of **1** (0.5 g, 1.03 mmol), 4-(diethylamino)benzaldehyde (0.2 g, 1.13 mmol) was added and heated to reflux for 10 h. The reaction mixture was cooled to room temperature and the Schiff base thus formed was reduced with $NaBH_4$. After completion of the reduction, the solvent was evaporated to dryness under reduced pressure. Water (30 mL) was added and extracted with $CHCl_3$ (330 mL). The combined organic layers, after drying over anhydrous Na_2SO_4, were evaporated under reduced pressure to obtain a pale yellow semi-solid product, which was further purified by column chromatography ($CHCl_3$–MeOH = 97 : 3 v/v) to obtain **5** as a pale yellow solid. Yield: 0.49 g (74%); mp: 76 C; HR-MS(ESI$^+$), m/z^+ (%): 646.5386 [**5**+1]$^+$ (59%), calculated for $C_{41}H_{51}N_5O_2$ = 645.4043; ^{1}H-NMR (300 MHz, $CDCl_3$, 25 C, TMS, δ): 7.886 (d, J = 4.2 Hz, 1H), 7.414 (br s, 1H), 7.248 (br s, 1H), 7.021 (t, J = 8.7 Hz, 1H), 6.866 (d, J = 8.1 Hz, 2H), 6.557 (d, J = 8.1 Hz, 2H), 6.516 (s, 2H), 6.310–6.458 (m, 4H), 6.239 (d, J = 8.7 Hz, 2H), 6.078 (d, J = 8.4 Hz, 2H), 3.464 (s, 2H), 3.220–3.226 (m, 12H), 2.434 (t, J = 6.3 Hz, 2H), 2.132–2.310 (m, 2H), 1.964(s, 1H), 1.109–1.1777 (m, 18H); ^{13}C-NMR (100 MHz, $CDCl_3$, 25 C, TMS, δ): 168.72, 167.84, 153.84, 153.54, 153.42, 148.90, 146.79(d), 132.20(d), 131.74, 131.27, 130.16(d), 129.50, 129.13, 128.89, 128.10, 126.83, 126.29, 123.91, 122.89, 111.95(t), 108.03(d), 106.06, 105,71, 97.96, 65.02(d), 61.13, 56.02, 52.85, 51.59, 47.59, 44.52, 41.14, 40.16, 38.25, 12.76; anal. calcd for $C_{41}H_{51}N_5O_2$: C, 76.24, H, 7.96, N, 10.84%; found: C, 76.11, H, 8.03, N 10.77%.

Compound 6. To a stirring ethanolic (40 mL) solution of **1** (0.5 g, 1.03 mmol), 4-(*N*,*N*-bis(2-hydroxyethyl)amino)-benzaldehyde (0.3 g, 1.19 mmol) was added and allowed to react under reflux condition for 8 h. The reaction mixture was cooled to room temperature and the Schiff base thus formed was reduced with $NaBH_4$. After completion of the reduction, the solvent was evaporated to dryness under reduced pressure. The solid residual mass was added with water (30 mL) and extracted with $CHCl_3$ (330 mL). The combined organic layers, after drying over anhydrous Na_2SO_4, were evaporated under reduced pressure to obtain a pale yellow semi-solid product, which was further purified by column chromatography ($CHCl_3$–MeOH = 95 : 5 v/v) to obtain **6** as a yellowish-pink solid. Yield: 0.5 g (72%); mp: 86 C; ESI-MS, m/z^+ (%): 679.62 [**6**+1]$^+$ (48%); ^{1}H-NMR (300 MHz, $CDCl_3$, 25 C, TMS, δ): 7.880 (d, J = 2.7 Hz, 1H), 7.432 (t, J = 4.2 Hz, 2H), 7.046 (d, J = 8.4 Hz, 3H), 6.572 (d, J = 8.4 Hz, 2H), 6.410 (s, 1H), 6.369 (d, J = 2.7 Hz, 3H), 6.236–6.271 (dd, J = 6.9 Hz, J = 1.8 Hz, 2H), 3.786 (t, J = 4.2 Hz, 4H), 3.485–3.530 (dd, J = 6.0 Hz, J = 4.2 Hz, 6H), 3.341 (t, J = 7.2 Hz, 10H), 2.836 (br s, 2H), 2.434 (t, J = 6.0 Hz, 2H), 1.256 (s, NH), 1.159 (t, J = 6.9 Hz, 12H); ^{13}C-NMR (300 MHz, $CDCl_3$, 0 C, TMS, δ): 169.14, 153.85, 153.48, 149.02, 147.39, 132.76, 131.00, 129.81, 128.82, 128.29, 124.02, 122.99, 112.65, 108.41, 105.36, 98.01, 65.48, 60.68, 55.41, 52.38, 47.43, 44.57, 39.79, 29.89, 12.80; anal. calcd for $C_{41}H_{51}N_5O_4$: C, 72.64, H, 7.58, N, 10.33%; found: C, 72.55, H, 7.69, N 10.26%.

Acknowledgements

BPB wishes to thank the Department of Science and Technology, New Delhi, for the financial support (SR/FTP/CS-138/2006) for this work. The authors sincerely wish to thank the Director, IMMT for a CSIR-diamond jubilee research internship to AP.

References

1 D. Beyersmann, in *Metals and their compounds in the environment*, E. Merian, (ed.), Wiley-VCH, Weinheim, 1990.
2 (*a*) *Heavy Metals in the Environment*, B. Sarkar, ed., Marcel Dekker, Inc., New York, 2002; (*b*) *Clinical Environmental Health and Toxic Exposure*, J. B. Sullivan and G. R. Kriger, ed., 2nd edn, Lippincott Williams and Wilkins, Philadephia, 2001.
3 For reviews, see: (*a*) J. S. Kim and D. T. Quang, *Chem. Rev.*, 2007, **107**, 3780; (*b*) B. Bag and P. K. Bharadwaj, in *Photo Electrochemistry & Photobiology in the Environment Energy and Fuel*, S. Kaneco, ed., 2007, 201; (*c*) V. Amendola, L. Fabbrizzi, F. Forti, M. Licchelli, C. Mangano, P. Pallavicini, A. Poggi, D. Sacchi and A. Taglieti, *Coord. Chem. Rev.*, 2006, **250**, 273; (*d*) J. F. Callan, A. P. de Silva and D. C. Magri, *Tetrahedron*, 2005, **61**, 8551; (*e*) V. Amendola, L. Fabbrizzi, F. Forti, M. Licchelli, C. Mangano, P. Pallavicini, A. Poggi, D. Sacchi and A. Taglieti, *Coord. Chem. Rev.*, 2006, **250**, 273; (*f*) K. Rurack, *Spectrochim. Acta*, 2001, **57A**, 2161; (*g*) B. Valeur and I. Leray, *Coord. Chem. Rev.*, 2000, **205**, 3; (*h*) A. P. de Silva, H. Q. N. Gunaratne, T. Gunnlauggsson, A. J. M. Huxley, C. P. McCoy, J. T. Radmacher and T. E. Rice, *Chem. Rev.*, 1997, **97**, 1515.
4 (*a*) M. Beija, C. A. M. Afonso and J. M. G. Martinho, *Chem. Soc. Rev.*, 2009, **38**, 2410; (*b*) H. N. Kim, M. H. Lee, H. J. Kim, J. S. Kim and J. Yoon, *Chem. Soc. Rev.*, 2008, **37**, 1465.
5 (*a*) Y. Zhou, X.-Y. You, Y. Fang, J.-Y. Li, K. Liu and C. Yao, *Org. Biomol. Chem.*, 2010, **8**, 4819; (*b*) Y. Zhao, Y. Sun, X. Lv, Y. Liu, M. Chen and W. Guo, *Org. Biomol. Chem.*, 2010, **8**, 4143; (*c*) W. Lin, X. Cao, Y. Ding, L. Yuan and Q. Yu, *Org. Biomol. Chem.*, 2010, **8**, 3618; (*d*) Z.-Q. Hu, C.-S. Lin, X.-M. Wang, L. Ding, C.-L. Cui, S.-F. Liu and H. Y. Lu, *Chem. Commun.*, 2010, **46**, 3765; (*e*) W. Lin, X. Cao, Y. Ding, L. Yuan and L. Long, *Chem. Commun.*, 2010, **46**, 3529; (*f*) W. Shi, S. Sun, X. Li and H. Ma, *Inorg. Chem.*, 2010, **49**, 1206; (*g*) J. Hu, C. Li and S. Liu, *Langmuir*, 2010, **26**, 724; (*h*) S. K. Kim, K. M. K. Swamy, S.-Y. Chung, H. N. Kim, M. J. Kim, Y. Jeong and J. Yoon, *Tetrahedron Lett.*, 2010, **51**, 3286; (*i*) W. Liu, L. Xu, H. Zhang, J. You, X. Zhang, R. Sheng, H. Li, S. Wu and P. Wang, *Org. Biomol. Chem.*, 2009, **7**, 660; (*j*) W. Huang, C. Song, C. He, G. Lv, X. Hu, X. Zhu and C. Duan, *Inorg. Chem.*, 2009, **48**, 5061; (*k*) J. Huang, Y. Xu and X. Qian, *J. Org. Chem.*, 2009, **74**, 2167; (*l*) M. H. Lee, S. W. Lee, S. H. Kim, C. Kang and J. S. Kim, *Org. Lett.*, 2009, **11**, 2101; (*m*) M. Suresh, S. Mishra, S. K. Mishra, E. Suresh, A. K. Mandal, A. Shrivastav and A. Das, *Org. Lett.*, 2009, **11**, 2740; (*n*) M. Zhu, C. Zhou, Y. Zhao, Y. Li, H. Liu and Y. Li, *Macromol. Rapid Commun.*, 2009, **30**, 1339; (*o*) S. K. Kwon, H. N. Kim, J. H. Rho, K. M. K. Swamy, S. M. Shanthakumar and J. Yoon, *Bull. Korean Chem. Soc.*, 2009, **30**, 719; (*p*) P.-x. Xi, L. Huang, H. Liu, P.-f. Jia, F,-j. Chen, M. Xu and Z.-z. Zeng, *JBIC, J. Biol. Inorg. Chem.*, 2009, **14**, 815; (*q*) P. Zhou, Q. Meng, G. He, H. Wu, C. Duan and X. Quan, *J. Environ. Monit.*, 2009, **11**, 648; (*r*) W. Huang, P. Zhou, W. Yan, C. He, L. Xiong, F. Li and C. Duan, *J. Environ. Monit.*, 2009, **11**, 330; (*s*) X. Zhang, Y. Xiao and X. Qian, *Angew. Chem., Int. Ed.*, 2008, **47**, 8025; (*t*) W. Shi and H. Ma, *Chem. Commun.*, 2008, 1856; (*u*) X. Q. Zhan, Z. H. Qian, H. Zheng, B.-Y. Su, Z. Lan and J. G. Xu, *Chem. Commun.*, 2008, 1859; (*v*) D. Wu, W. Huang, Z. Lin, C. Duan, C. He, S. Wu and D. Wang, *Inorg. Chem.*, 2008, **47**, 7190; (*w*) M. Yuan, W. Zhou, X. Liu, M. Zhu, J. Li, X. Yin, H. Zheng, Z. Zuo, C. Ouyang, H. Liu, Y. Li and D. Zhu, *J. Org. Chem.*, 2008, **73**, 5008; (*x*) K. N. Kim, M. G. Choi, J. H. Noh, S. Ahn and S.-K. Chang, *Bull. Korean Chem. Soc.*, 2008, **29**, 571.
6 (*a*) X. Chen, S.-W. Nam, M. J. Jou, Y. Kim, S.-J. Kim, S. Park and J. Yoon, *Org. Lett.*, 2008, **10**, 5235; (*b*) M. G. Choi, D. H. Ryu, H. L. Jeon, S. Cha, J. Cho, H. H. Joo, K. S. Hong, C. Lee, S. Ahn and S.-K. Chang, *Org. Lett.*, 2008, **10**, 3717; (*c*) M. H. Lee, J.-S. Wu, J. W. Lee,

J. H. Jung and J. S. Kim, *Org. Lett.*, 2007, **9**, 2501; (*d*) J.-S. Wu, I. C. Hwang, K. S. Kim and J. S. Kim, *Org. Lett*., 2007, **9**, 907; (*e*) H. Yang, Z. Zhou, K. Huang, M. Yu, F. Li, T. Yi and C. Huang, *Org. Lett.*, 2007, **9**, 4729; (*f*) A. B. Othman, J. W. Lee, J.-S. Wu, J. S. Kim, R. Abidi, P. Thuery, J. M. Strub, A. V. Dorsselaer and J. Vicens, *J. Org. Chem.*, 2007, **72**, 7634; (*g*) M. H. Lee, S. J. Lee, J. H. Jung, H. Lim and J. S. Kim, *Tetrahedron*, 2007, **63**, 12087; (*h*) D. Wu, W. Huang, C. Duan, Z. Lin and Q. Meng, *Inorg. Chem.*, 2007, **46**, 1538; (*i*) J. H. Soh, K. M. K. Swamy, S. K. Kim, S. Kim, S.-H. Lee and J. Yoon, *Tetrahedron Lett.*, 2007, **48**, 5966; (*j*) X. Zhang, Y. Shiraishi and T. Hirai, *Tetrahedron Lett.*, 2007, **48**, 5455; (*k*) S.-K. Ko, Y.-K. Yang, J. Tae and I. Shin, *J. Am. Chem. Soc.*, 2006, **128**, 14150; (*l*) H. Zheng, J. H. Qian, L. Xu, F. F. Yuan, L.-D. Lan and J. G. Xu, *Org. Lett.*, 2006, **8**, 859; (*m*) Y.-K. Yang, K.-J. Yook and J. Tae, *J. Am. Chem. Soc.*, 2005, **127**, 16760; (*n*) C.-C. Huang and H.-T. Chang, *Anal. Chem.*, 2006, **78**, 8332.

7 Y. Shiraishi, S. Sumiya, Y. Kohno and T. Hirai, *J. Org. Chem.*, 2008, **73**, 8571.

8 (*a*) Y. Liu, Y Sun, J. Du, X. Lv, Y. Zhao, M. Chen, P. Wang and W. Guo, *Org. Biomol. Chem.*, 2011, **9**, 432; (*b*) W. Lin, L. Long, B. Chen, W. Tan and W. Gao, *Chem. Commun.*, 2010, **46**, 1311; (*c*) C. Yu, J. Zhang, R. Wang and L. Chen, *Org. Biomol. Chem.*, 2010, **8**, 5277; (*d*) L. Huang, X. Wang, G. Xie, P. Xi, Z. Li, M. Xu, Y. Wu, D. Bai and Z. Zeng, *Dalton Trans.*, 2010, **39**, 7894; (*e*) C. Kaewtong, J. Noiseephum, Y. Uppa, N. Morakot, N. Morakot, B. Wanno, T. Tuntulani and B. Pulpoka, *New J. Chem.*, 2010, **34**, 1104; (*f*) F. Yu, W. Zhang, P. Li, Y. Xing, L. Tong, J. Ma and B. Tang, *Analyst*, 2009, **134**, 1826; (*g*) Y. Zhao, X.-B. Zhang, Z.-X. Han, L. Qiao, C.-Y. Li, L.-X. Jian, G.-L. Shen and R.-Q. Yu, *Anal. Chem.*, 2009, **81**, 7022; (*h*) Y. Zhou, F. Wang, Y. Kim, S.-J. Kim and J. Yoon, *Org. Lett.*, 2009, **11**, 4442; (*i*) K. M. K. Swamy, S.-K. Ko, S. K. Kwon, H. N. Lee, C. Mao, J.-M. Kim, K.-H. Lee, J. Kim, I. Shin and J. Yoon, *Chem. Commun.*, 2008, 5915; (*j*) M. H. Lee, H. J. Kim, S. Yoon, N. Park and J. S. Kim, *Org. Lett.*, 2008, **10**, 213; (*k*) X. Zhang, Y. Shiraishi and T. Hirai, *Org. Lett.*, 2007, **9**, 5039; (*l*) Y. Xiang, A. Tong, P. Jin and Y. Ju, *Org. Lett.*, 2006, **8**, 2863; (*m*) V. Dujols, F. Ford and A. W. Czarnik, *J. Am. Chem. Soc.*, 1997, **119**, 7386.

9 (*a*) M. H. Lee, T. V. Giap, S. H. Kim, Y. H. Lee, C. Kang and J. S. Kim, *Chem. Commun.*, 2010, **46**, 1407; (*b*) M. Xu, S. Wu, F. Zeng and C. Yu, *Langmuir*, 2010, **26**, 4529; (*c*) J. Mao, Q. Heb and W. Liu, *Talanta*, 2010, **80**, 2093; (*d*) X. Zhang, Y. Shiraishi and T. Hirai, *Tetrahedron Lett.*, 2008, **49**, 4178; (*e*) M. Zhang, Y. Gao, M. Li, M. Yu, F. Li, L. Li, M. Zhu, J. Zhang, T. Yia and C. Huang, *Tetrahedron Lett.*, 2007, **48**, 3709; (*f*) L. Zhang, J. Fan and X. Peng, *Spectrochim. Acta, Part A*, 2009, **73**, 398; (*g*) S. Bae and J. Tae, *Tetrahedron Lett.*, 2007, **48**, 5389; (*h*) J. Mao, L. Wang, W. Dou, X. Tang, Y. Yan and Weisheng Liu, *Org. Lett.*, 2007, **9**, 4567; (*i*) Y. Xiang and A. Tong, *Org. Lett.*, 2006, **8**, 1549.

10 (*a*) Z. Zhou, M. Yu, H. Yang, K. Huang, F. Li, T. Yi and C. Huang, *Chem. Commun.*, 2008, 3387; (*b*) K. Huang, H. Yang, Z. Zhou, M. Yu, F. Li, X. Gao, T. Yi and C. Huang, *Org. Lett.*, 2008, **10**, 2557.

11 Y. Kwon, Y. J. Jang, Y. J. Lee, K. M. Kim, M. S. Seo, W. Nam and J. Yoon, *J. Am. Chem. Soc.*, 2005, **127**, 10107.

12 (*a*) O. A. Egorova, H. Seo, A. Chatterjee and K. H. Ahn, *Org. Lett.*, 2010, **12**, 401; (*b*) Y.-K. Yang, S. Lee and J. Tae, *Org. Lett.*, 2009, **11**, 5610.

13 H. Li, J. Fan, J. Du, K. Guo, S. Sun, X Liu and X. Peng, *Chem. Commun.*, 2010, **46**, 1079.

14 G. He, D. Guo, C. He, X. Zhang, X. Zhao and C. Duan, *Angew. Chem., Int. Ed.*, 2009, **48**, 6132.

15 (*a*) W. F. Fitzgerald, C. H. Lamborg and C. R. Hammerschmidt, *Chem. Rev.*, 2007, **107**, 641; (*b*) W. F. Fitzgerald, D. R. Engstrom, R. P. Mason and E. A. Nater, *Environ. Sci. Technol.*, 1998, **32**, 1.

16 (*a*) A. Renzoni, F. Zino and E. Franchi, *Environ. Res.*, 1998, **77**, 68; (*b*) O. Malm, *Environ. Res.*, 1998, **77**, 73; (*c*) P. Grandjean, P. Weihe, R. F. White and F. Debes, *Environ. Res.*, 1998, **77**, 165; (*d*) M. Harada, *Crit. Rev. Toxicol.*, 1995, **25**, 1.

17 M. Shamsipur, M. Hosseini, K. Alizadeh, N. Alizadeh, A. Yari, C. Caltagirone and V. Lippolis, *Anal. Chim. Acta*, 2005, **533**, 17.

18 *Gaussian 09, G09W*, Gaussian Inc., Wallingford, USA, 2009.

19 X. Qi, E. J. Jun, L. Xu, S.-J. Kim, J. S. J. Hong, Y. J. Yoon and J. Yoon, *J. Org. Chem.*, 2006, **71**, 2881.

20 W. F. L. Armarego and D. D. Perrin, *Purification of laboratory chemicals*, 4th edn, Butterworth-Heinemann, Oxford, 1997.

21 B. Bag and A. Pal, *Org. Biomol. Chem.*, 2011, **9**, 915.

22 M. Fischer and J. Georges, *Chem. Phys. Lett.*, 1996, **260**, 115.

23 C. R. Lohani, J.-M. Kim, S.-Y. Chung, J. Yoon and K.-H. Lee, *Analyst*, 2010, **135**, 2079.

